의학박사 학위논문

A study on the features of memory impairment and neuropathology in crossbreed mice of Tg2576 and S100A9 knockout mice model

S100A9 knockout 마우스와 알츠하이머질환 마우스 교배 모델에서 기억력 손상과 신경병리학적인 특징에 관한 연구

2014 년 02 월

서울대학교 대학원
의과학과 박사과정
김 희 진

A thesis of the Degree of Doctor of Philosophy
in Medical Science

S100A9 knockout 마우스와 알츠하이머질환 마우스 교배 모델에서 기억력 손상과 신경병리학적인 특징에 관한 연구

A study on the features of memory impairment and neuropathology in crossbreed mice of Tg2576 and S100A9 knockout mice model

Feb 2014

The Department of Biomedical Sciences,
Seoul National University
College of Medicine
Hee Jin Kim

A study on the features of memory impairment and neuropathology in crossbreed mice of Tg2576 and S100A9 knockout mice model

by
Hee Jin Kim

A thesis submitted to the Department of Biomedical Science in partial fulfillment of the requirement of the Degree of Doctor of Philosophy in Medical Sciences at Seoul National University College of Medicine

Feb. 2014

Approved by Thesis Committee:

Professor Chairman
Professor Vice chairman
Professor
Professor
Professor

ABSTRACT

Our previous study presented evidence that the inflammation-related S100A9 gene is significantly upregulated in the brains of Alzheimer's Disease (AD) animal models and human AD patients. In addition, experiments have shown that knockdown of S100A9 expression improves cognition function in AD model mice (Tg2576), and these animals exhibit reduced amyloid plaque burden.

In this study, I established a new transgenic animal model of AD by crossbreeding Tg2576 mouse with the S100A9 knockout (KO) mouse. I observed that S100A9 KO/Tg2576 (KO/Tg) mice displayed an increased spatial reference memory in Morris water maze and Y-maze tasks as well as decreased amyloid beta peptide (Aβ) neuropathology because of reduced levels of Aβ, C-terminal fragments of APP (APP-CT) and phosphorylated tau and increased expression of anti-inflammatory IL-10 and also decreased expression of inflammatory IL-6 and tumor neurosis factor (TNF)-α when compared with age-matched S100A9 WT/Tg2576 (WT/Tg) mice.

Overall, these results suggest that S100A9 is responsible for the neurodegeneration and cognitive deficits in Tg2576 mice. The mechanism of S100A9 is able to coincide with the process of inflammatory cytokines. These findings indicate that knockout of S100A9 is a potential target for the pharmacological therapy of AD.

Keywords: Alzheimer's disease, S100A9, knockout, inflammation

Student number: 2010-30608

CONTENTS

LIST OF TABLES AND FIGURES

LIST OF ABBREVIATIONS

Aβ, amyloid beta peptide

AD, Alzheimer 's disease

APP, Amyloid precursor protein

APP-CT, C-Terminal fragment of APP

FC, Frontal cortex

HT, Hetero type

IL, Interleukin

KO, Knockout

PBS, Phosphate-buffered saline

PC, Parietal cortex

Tg, Tg2576

TNF-α, tumor necrosis factor-α

WT, Wild type

INTRODUCTION

The S100 protein family represents the largest sub group within the Ca^{2+} binding EF-hand superfamily (1). As S100 proteins have diverse functions, it is not surprising that these proteins are implicated in numerous human diseases, including different types of cancer characterized by altered expression levels of S100 proteins as well as inflammatory and autoimmune diseases (1,2). Some S100 proteins, such as S100A6 and S100B, play a prominent role in neurodegenerative disorders, including Alzheimer's disease (AD) (1,3,4,5,6).

In a recent study on the pro-inflammatory S100A8/A9 proteins, amyloid formation was formed in the aging prostate (7), and previous experiments in our laboratory have demonstrated that S100A9 plays a prominent role in AD (8).

Inflammation, insoluble protein deposition and neuronal cell loss are important features of the AD brain. S100A9, a the member of the calcium binding S100 protein family that is also known as MRP14 or Calgranulin B, is an inflammation-associated protein that is constitutively expressed in neutrophils and inducible in numerous inflammatory cells, including macrophages, epithelial cells, and keratinocytes (9,10,11). S100A9 plays a role in the

inflammation of the AD brain; however, a detailed mechanism has not been sufficiently reported.

Neuronal degeneration, which involves synaptic and neuronal loss, and formations of intracellular neurofibrillary tangles and extracellular neuritic plaques containing amyloid beta peptide (Aβ) plays a central role in the pathogenesis of neurodegenerative diseases, particularly in AD (12, 13, 14). The enzymes, β- and γ-secretase generate monomeric Aβ in neurons from APP (15). Monomeric Aβ undergoes conformational transitions and forms a dimer or trimer as well as soluble high molecular weight aggregates, and it progresses to form spherical oligomers that are composed of 12 to 24 monomers. Protofibrils elongated by these oligomers become insoluble fibrils (16,17). Many researchers have reported that the presence of oligomeric Aβ is more strongly correlated with disease symptoms than amyloid plaques (15,17,18,19). And aggregates of Aβ have also been shown to activate microglia and induced the production of pro-inflammatory cytokines such as tumor necrosis factor (TNF)-α, Interleukins-6 (IL-6) (13, 20)and reduced the production of anti-inflammatory cytokine such as IL-10(21).

It is well known that Tg2576 mice harboring the human APP transgene with the familial AD Swedish mutation develop AD-like cerebral amyloidosis (22,23). Under 6month of age, the mice have normal memory and lack neuropathology; at 6-13 months, the mice develop memory deficits without neuronal loss; and in mice older than 14 months, neuritic plaques containing Aβ form (24,25,26,27). There is strong evidence that Aβ is responsible for the age-related memory decline (28,29,27). In addition, Tg2576 mice develop age-dependent behavioral deficits when studied using the Y-maze and Morris water maze test (24,26,27).

There have been many recent studies that have examined S100A9 deficiencies. For example, in one study, S100A9 deficient mice were used to confirm the expression of IL-8-induced CD11b (30). In another study, S100A9-deficient mice were used as a model to study the role of two S100 proteins in calcium and zinc metabolism in neutrophils (10). However, these studies were not related to AD.

To assess whether S100A9 knockout rescued the cognitive deficit and neuropathology in AD animal mice, S100A9 KO mice were crossbred with Tg2576 mice. These mice allowed for the

comparison of four groups of mice; Wild type/Wild type (WT/WT), S100A9 Knock out/Wild type (KO/WT), Wild type/Tg2576 (WT/Tg), and S100A9 Knock out/Tg2576 (KO/Tg). At 13 months of age, I found that KO/Tg mice showed rescued cognitive impairments compared to WT/Tg mice. I also confirmed differences in pathogenesis, particularly abundant amyloid neuritic plaques containing Aβand phosphorylated tau proteinsand inflammatory process relatedcytokines in4 groups of 14-month-old100A9 KO/Tg crossbred mice.

MATERIALS AND METHODS

1. Generation of S100A9 KOxTg crossbred mice and genotyping by PCR

All animal procedures were performed following the National Institutes of Health Guidelines for the Humane Treatment of Animals, with approval from the Institutional Animal Care and Use Committee of Seoul National University (IACUC No. SNU-100611-1). Animals of only male were used in this study.

S100A9 KO mice in a C57BL/6 background were kindly provided by Wolfgang Nacken (Münster University, Germany) (30) and crossed with Tg2576 mice expressing human APP695 with the Swedish mutation (K670N/M671L) on a C57BL/6/SJL background. Tg2576 mice were obtained from Taconic Farms (Germantown, NY) and were bred by mating male mice with C57BL6/SJL F1 females, as described by others (26).

To analyze the offspring, genomic DNA samples isolated from mice tails was genotyped based on the previously

described method (8,26). Four different genotypes (WT/WT, KO/WT, WT/Tg, KO/Tg) were studied at 14 months of age (9~15 mice per group).

2. Tissue preparation

To obtain tissues for experiments, the animals were anaesthetized and immediately cardiac-perfused with PBS containing heparin. For morphological analyses, one hemisphere of the brain was fixed in a 4 % paraformaldehyde solution for 24 h, incubated in 30 % sucrose for 72 h at 4°C and embedded in paraffin. For biochemical analyses, including Western blotting, enzymatic activity assays and enzyme-linked immunosorbent assays, the other half of the brain was quickly frozen on dry ice and stored at −70°C. Tissues were lysed in RIPA buffer with protease inhibitors cocktail (Roche).

3. Immunohistochemistry

Sections were deparaffinized in 60°C for 1 h in xylene and dehydrated using graded alcohols to water. Sections were retrieved by 0.01 M citric acid (pH 6.0) and blocked with 0.5 % triton X-100 and 2 % normal serum in TBS. Appropriate primary antibodies were incubated overnight and were visualized using an appropriate secondary antibody. For labeling, immunohistochemistry was performed using a Vectastain avidin biotin complex (ABC) elite kit. The reaction product was detected using 3.3-diaminobenzidinetetrahydrochloride (DAB).

4. Western blot

Tissues were washed with phosphate-buffered saline (PBS) and lysed in RIPA buffer with a cocktail of protease inhibitors (Roche). Proteins were separated using SDS-PAGE and transferred to a PVDF membrane. The PVDF membrane was blocked with 5 % nonfat dry milk in Tris-Buffered Saline containing 0.05 % Tween 20 (TBS-T). After 1 h of blocking, the protein blot was confirmed using

appropriate antibodies at 4°C overnight and detected using a horseradish peroxidase-conjugated secondary antibody (Amersham Pharmacia). Westen blotting was detected by Gel doc system (Bio-rad) and data was analyzed using quantity one program (bio-rad).

5. Antibodies

The following primary antibodies were used: anti-Aβ mouse monoclonal antibody 6E10 (MAB5206; Chemicon), anti-mouse S100A9 and S100A8 (AF2065, AF3059; R&D systems), S100B (ab52642; Abcam), GAPDH (Abfrontier), anti-Amyloid Oligomer, Aβ, (AB9234; Millipore), Calnexin (H-70) (sc-11397;Santa Cruz Biotechnology), and p-Tau (Ser404) (sc-12952; Santa Cruz Biotech.).

6. ELISA

ELISAs were performed using colorimetric sandwich ELISAs kits (human amyloid-beta ($A\beta_{1-42}$): IBL, mouse IL-10: KMC0102, Invitrogen, mouse IL-6: DY406, R&D

systems, TNF-α: DY410, R&D systems) for the quantitative determination of human $A\beta_{1-42}$, IL-10, IL-6, and TNF-α in brains. All assays were performed according to manufacturer's specific instructions. Levels of these proteins were calculated from a standard curve developed with specific OD versus serial dilutions of known concentration. Each standard and experimental sample was run in duplicate, and the results were averaged.

7. Morris water maze task

The Morris water maze was performed at 13 months after birth to measure spatial reference learning and memory based on the previously described method (8). A training session consisted of a series of three trials per day for 5 consecutive days and a single probe trial was conducted 48hrs after the final training session,

8. Y-maze task

Spatial memory was assessed using Y-maze test. The apparatus consisted of a black plastic maze with three arms that intersected at 120° (60 cm long, 15 cm high and 10 cm wide). Vertical metal poles located at the outer perimeter of the maze provided spatial cues. A mouse was placed at the end of one arm and allowed to move freely through the maze for 8 min without reinforcements, such as, food and water. The total numbers of entries into the arms, including returns to the same arms, was recorded. Alternation was defined as entry into each of the three arms consecutively. The maximum number of alternations was calculated by subtracting two from the total number of arms entered. Percent alternation was calculated by expressing actual alternations as a percentage of maximum alternations (31).

9. Passive avoidance test

As described previously (32, 33), the passive avoidance test apparatus (Model PACS-30, Columbus Instruments

Int.) was used to evaluate the effects of S100A9 KOxTg crossbred mice on learning and memory. The shuttle box is divided into two chambers of equal size (23.5 * 15.5 * 15.5 cm) separated by a guillotine door (6.5 * 4.5 cm). The light chamber is equipped and mice can enter the dark chamber through the guillotine door. Mice were initially placed in the light chamber with the door open. If the mice entered the dark compartment, the door closed automatically. Training was repeated until the mice entered the dark compartment within 30 sec (training trial). When mice entered the dark chamber, an electrical foot shock (0.3 mA) was delivered for 3 sec through the grid floor and the door was closed automatically (acquisition trial). The mice were replaced in the illuminated chamber 24 h after the acquisition trial and the latency period to enter the dark chamber was measured for 300 sec (retention trial). If a mouse did not enter the dark chamber within the cut-off time (300 sec), it was assigned a latency value of 300 sec.

10. Congo red staining

Brain sections (4 μm) were deparaffinized and hydrated using a descending ethanol series. After washing in a freshly prepared alkaline alcoholic saturated sodium chloride reagent (2.5 mM NaOH in 80 % reagent-grade alcohol) for 20 min at room temperature, the sections were incubated in 0.4 % Congo red (W/V, Sigma) in an alkaline alcoholic saturated sodium chloride reagent (freshly prepared and filtered prior to use) for 30 min at room temperature. Sections were washed in distilled water and counterstained with hematoxylin for 1 min. Sections were rinsed using ascending grades of ethanol with a final three changes of 100 % reagent-grade ethanol, cleared in xylene and cover slipped with per mount (Fisher Scientific) (31).

11. Secretase activity test

The fluorometric assay of secretase was conducted using β- and γ-secretase activity kits (R&D systems, Inc., USA) in accordance with the protocol supplied by the manufacturer. As an enzyme source, total cortical protein lysates were tested. Quantification of substrate cleavage was assessed using a fluorometric reader (355nm excitation, 510nm emission).

12. Statistical analysis

Data were expressed as the mean ±SEM value or as fraction of the control value ± SEM. Statistical analysis was performed using one-way ANOVA: Tukey's HSD Post Hoc test using PASW statistics (SPSS version 18). The difference was considered statistically significant for *, $p \leq 0.05$, **, $p \leq 0.01$, and ***, $p \leq 0.001$.

RESULTS

Generation of S100A9 KO/Tg2576 crossbred mice

To elucidate whether S100A9$^{-/-}$ plays a key role in AD progression, I crossbred F1 male S100A9$^{+/-}$/Tg2576 (HT/Tg) mice with female S100A9$^{+/-}$/WT (HT/WT) mice to generate F2 littermates with the following genotypes: S100A9$^{+/+}$/WT (WT/WT), HT/WT, S100A9$^{-/-}$/WT (KO/WT), S100A9$^{+/+}$/Tg2576 (WT/Tg), HT/Tg and S100A9$^{-/-}$/Tg2576 (KO/Tg) mice. The experimental groups included WT/WT, KO/WT, WT/Tg and KO/Tg. In Figure 2 and 3, the genotypes of mice from 4 groups were confirmed using PCR and Western blotting. I successfully obtained 4 discrete groups in the F2 littermates, as shown by the PCR and western blotting data. In immunohistochemical analysis, the S100A9 protein was significantly increased in the cortex and hippocampus of WT/Tg mice brains compared with region-matched WT/WT mice brains (Figure 4). There was no noticeable expression of S100A9in S100A9 KO/Tg mice brains but in WT/Tg mice brains (Figure 4).

I investigated the levels of other specific calcium-binding proteins, including calnexin, S100A8 and S100B in the brains of

S100A9 KO/Tg crossbred mice by Western blot analysis. My data indicate that there was no change in their levels among all groups (Figure 3). I also investigated S100A8 immuno – positive cells in the brains of S100A9 KO/Tg2576 crossbred mice using immunohistochemistry. Here, no differences in S100A8 expression in the brains of all groups were detected (Figure 3).

S100A9 KO/Tg2576 crossbred mice showed significant improvements in spatial reference memory

At 13 months of age, I evaluated learning and memory impairment in S100A9 KO/Tg2576 crossbred mice using the Morris water maze task. With trainings repeated every day, WT/WT, KO/WT and KO/Tg groups found the hidden platform with less movement, and the WT/Tg group wandered with no apparent pattern (Figure 5). On the 5th day of the learning sessions, analysis of the escape latency of each group showed significant differences between the KO/Tg and WT/Tg groups (Figure 5). I found no noticeable differences between the WT/WT and KO/Tg groups (Figure 5).

To confirm the memory impairment in WT/Tg mice, I performed the probe test 48 hr after the final trial and recorded the duration of time spent in zone 4 without the platform. Similar to the WT/WT group, the KO/Tg mice stayed significantly longer in zone 4 than the other zones (zones 1−3) (Figure 6). However, there was no significant difference for WT/Tg mice in terms of time spent in different zones, and no noticeable difference in the KO/WT mice (Figure 6).

Similar results were observed in the Y−maze test. The alternation rate of arm entries in the Y−maze test was similar in the WT/WT and KO/WT groups. The alteration rate of arm entries was significantly decreased in the WT/Tg group (P=0.009, F=54.8%) but not in the KO/Tg group (P=0.015, F=64.4%; Figure 7). These data show that knockout of S100A9 increased the spatial reference memory in KO/Tg mice.

To further examine the learning and memory function in S100A9 KO/Tg crossbred mice, I performed the passive avoidance test. As shown in Figure 8, the latency of the KO/Tg group was longer than the WT/Tg group in the passive avoidance test (P=0.003, F=106.6). In the analysis of these

behavioral test findings, the S100A9 KO/Tg crossbred mice showed an improvement in cognitive performance.

S100A9 KO/Tg2576 crossbred mice had the reduced number of amyloid plaques and decreased generation of $A\beta_{1-42}$.

Insoluble deposits of Aβ plaques are strong candidates for initiating the inflammatory response (11). The hippocampus and cortex, stained using Hematoxyline and Congo red, were used as a marker for the presence of amyloid (1,6).

In this study, I examined amyloid plaque load and protein levels of Aβ and APP-CT in the brains of 14-month-old WT/WT, KO/WT, WT/Tg and KO/Tg mice using Congo red staining and Western blot analysis with the 6E10 antibody, which specifically recognizes amino $acids_{1-17}$ of Aβ.

Congo red-stained fibrilar plaques were observed in the cortex and hippocampus in the brains of KO/Tg and WT/Tg mice (Figure 9). However, the number of amyloid plaques in KO/Tg mice was significantly reduced (from 17.7 to 10.5, P= 0.049, Student's t-test; Figure 10). In the brains of WT/WT and KO/WT mice, no amyloid plaques were observed (Figure 10).

Based on the Congo red staining data (Figure 9 and 10), I examined protein levels of amyloid precursor protein (APP), APP-CT and Aβ using the 6E10 antibody. The expression of APP was no different between the WT/Tg and KO/Tg groups; however, the levels of Aβ and APP-CT were decreased in the KO/Tg group (Figure 11), which is consistent with the decreased number of amyloid plaques. The levels of Aβ and APP-CT in the cortex of KO/Tg mice were significantly decreased (Aβ, from 1 to 0.43, P= 0.038; APP-CT, from 1 to 0.670, P=0.044; Figure 12 and 13).

Using Aβ ELISAs, I confirmed the $A\beta_{1-42}$ levels in the cortex and hippocampus of all groups. Similar to the Congo red staining and Western blot results, $A\beta_{1-42}$ in the brain of the KO/Tg group was significantly decreased by 51.17 % in the cortex (from 594.84 to 304.38, P=0.016; Figure 14) and 41.03 % in the hippocampus (from 250.8 to 102.9, P=0.047; Figure 15) compared to WT/Tg group.

Several studies have demonstrated that soluble Aβ oligomeric species can be extracted using saline buffers from the brain tissue of patients with AD, and the presence of soluble species is more strongly correlated with disease symptoms than

amyloid plaques (15, 18, 19). In the present study, oligomeric Aβ was detected by Western blot using a specific oligomeric Aβ antibody and quantified (Figure 16 and 17). In KO/Tg mice, I found a 0.47−fold decrease in oligomeric Aβ compared to the WT/Tg mice (P=0.031, Figure 17).

These data provide evidence that Aβ and APP−CT protein levels in the brain were reduced by knockout of S100A9.

S100A9KO/Tg2576 crossbred mice showed decreased phosphorylation of tau

Abnormal tau phosphorylation is known as a key hallmark of AD (34, 35,36,37,38). Accumulation of phosphorylated neurofilaments and phospho−tau occurs in neurites surrounded amyloid plaques in APP Tg mice (36,39,40,41,42).

To determine whether S100A9 causes hyperphosphorylation of tau, I performed immunohistochemistry using brain sections with a phospho−specific tau antibody directed to Ser 404 phosphorylation. Phosphorylated tau, detected near Aβ plaques was reduced in the hippocampus and cortex of KO/Tg mice brains (Figure 19).

These data showed that the S100A9 knockout functionally recovered the pathological deficits in Tg2576 mice.

The release of anti-inflammatory cytokine, IL-10 was increased and the release of pro-inflammatory cytokines, IL-6 and TNF-α were decreased in S100A9KO/Tg2576 crossbred mice

S100 proteins, including S100A8, S100A9 and S100A12, are known to contribute to chronic inflammation (43). Our previous study showed that treatment with si-S100A9 attenuated the increase of IL-1β, TNF-α and iNOS by APP-CT. The induction of NO by APP-CT was greatly reduced by si-S100A9 treatment, which suggest that S100A9 might induce neuroinflammation by increasing $[Ca^{2+}]_i$ levels (Ha et al. 2010). Therefore, I focused on the mechanism related to inflammatory cytokines.

IL-10, an anti-inflammatory cytokine, has been known to have an ameliorative effect on severe inflammation by inhibiting the production of IL-12, IL-6, IFN-γ and TNF-α (21). I confirmed the levels of cytokine in the total lysates from all

groups of mice brains. In the cortex of S100A9 KO/Tg mice brains, IL-10 was increased (from 58.68 pg/ml to 80.37 pg/ml, P=0.04) compared to WT/Tg mice (Figure 20). These data indicate that a deficiency of S100A9 might inhibit severe inflammation by increasing the expression of anti-inflammatory cytokines.

IL-6 and TNF-α, which are representative pro-inflammatory cytokines, were found to be induced in reactive astrocytes surrounding beta-amyloid deposits detected in 14-month-old Tg2576 mice(44). In KO/Tg mice brain,IL-6was significantly decreased (from 151.4pg/ml to 128.1pg/ml, P=0.048) compared to WT/Tg mice (Figure 21). And TNF-α, was also known for pro-inflammatory cytokine, was slightly decreased (from 136.2 pg/ml to 125.4 pg/ml, P=0.035) compared to WT/Tg mice (Figure 22). These data indicate that a deficiency of S100A9 might inhibit severe inflammation by increasing the expression of anti-inflammatory cytokines and by decreasing the expression of pro-inflammatory cytokines.

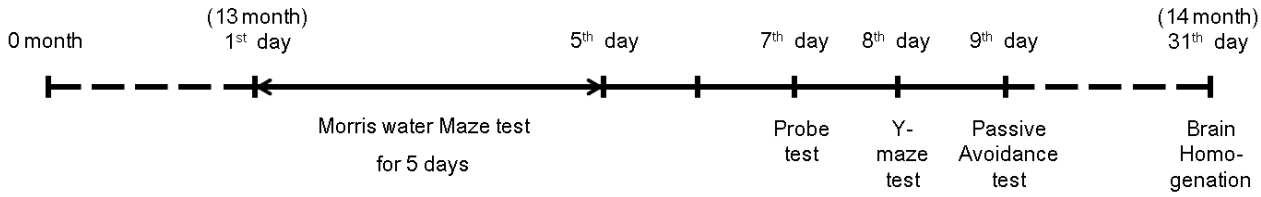

Figure 1.Test schedule

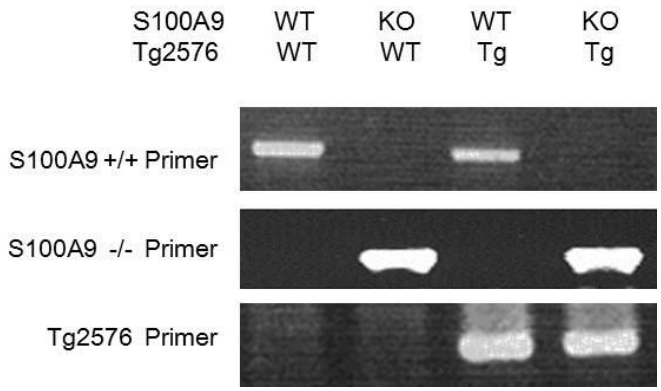

Figure 2.Genotyping was determined in the tails of WT/WT, KO/WT, WT/Tg and KO/Tg mice

For genotyping, DNA levels of S100A9 and Swedish APP were measured in each group by PCR analysis with each primer ($S100A9^{+/+}$ for WT of S100A9 and $S100A9^{-/-}$ for KO of S100A9; Tg2576 for Swedish form of APP). The absence of S100A9 was shown in KO/WT and KO/Tg mice and the DNA band of Swedish APP was detected in WT/Tg and KO/Tg mice. Actin was used as a loading control.

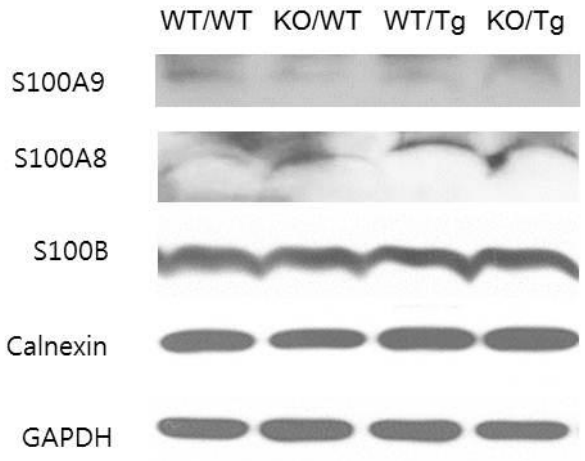

Figure 3.Protein expression in the brains ofS100A9 KO/Tg mice

At the age of 14-month, Western blot analysis was performed with the total lysate from the cortical region and hippocampal region of the brains from each group using an anti-S100A9 antibody. S100A9 expression was reduced in S100A9 KO mice, which was determined using the anti-S100A9 antibody. The levels of other calcium binding proteins including S1008, S100B, and Calnexin were investigated in the brain of S100A9 KO/Tg mice by Western blot. The membrane was stripped and reproved with GAPDH to confirm equal loading. There were no noticeable differences among all groups. This is a representative blot from at least five independent experiments.

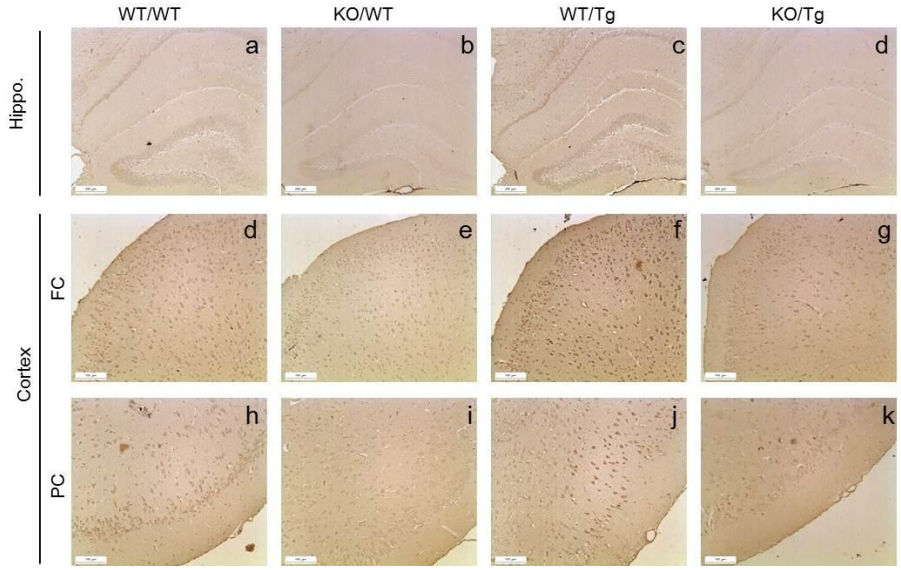

Figure 4. Immunohistochemistry of S100A9 in S100A9 KO/Tg mice

At the age of 14-months, S100A9 expression was observed in the brain by immunohistochemisty using the anti-S100A9 antibody. In the hippocampus and cortex of mice brain, S100A9 expression was significantly reduced in KO/Tg mice compared with WT/Tg mice. Significant differences were observed in the Frontal Cortex (FC) and Parietal Cortex (PC). Sections are 4 μm thick. Scale bar; 200 μm.

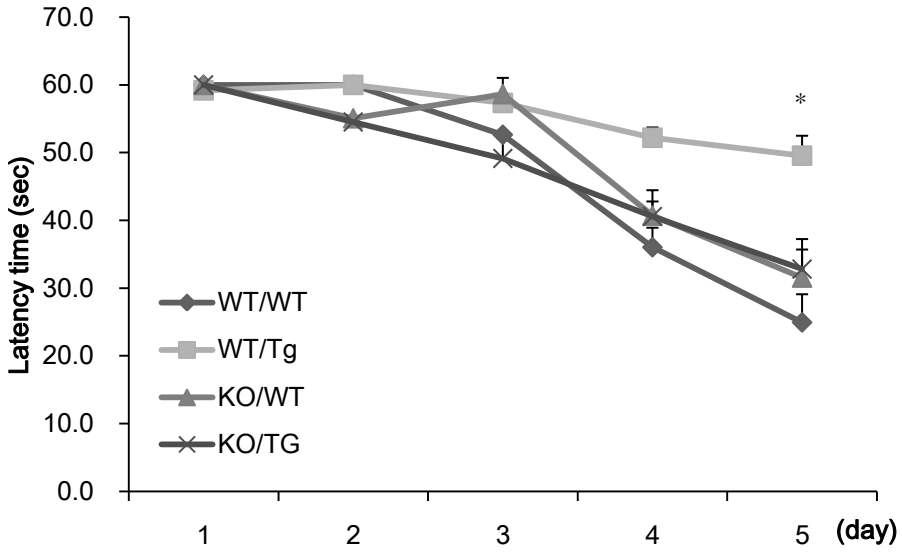

Figure 5. S100A9 KO/Tg crossbred mice showed significant improvement in spatial reference memory

I performed memory test at the age of 13-months. The water maze test was performed. Training trials were conducted for 5 consecutive days. From the 5th day of training trials, escape latency was significantly increased in the WT/Tg group. However, the latency was decreased in the KO/Tg group compared to the WT/Tg group. $*P<0.05$ by one-way ANOVA.

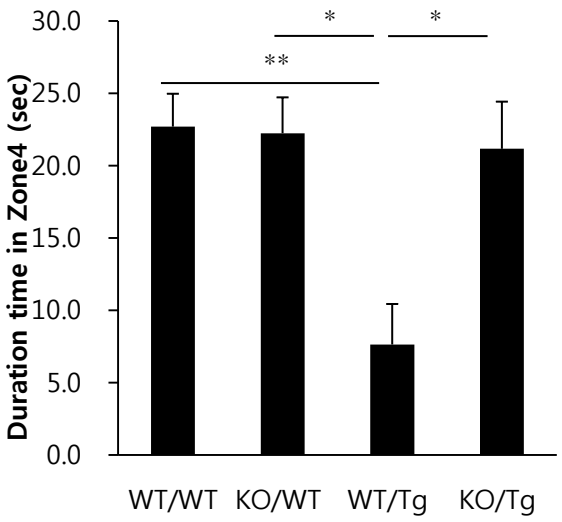

Figure 6. S100A9 KO/Tg crossbred mice showed significant improvement in probe test.

The probe test was performed 48h after the final training session. The times that the mice of each group stayed in zones 1, 2, 3 and 4 were compared. The time spent in the platform quadrant (zone 4) was significantly decreased in the Tg-sham group. However, the KO/Tg group showed memory improvement compared to the WT/Tg group in zone 4. (n=7-11) $*P<0.05$, $**P<0.01$ by one-way ANOVA.

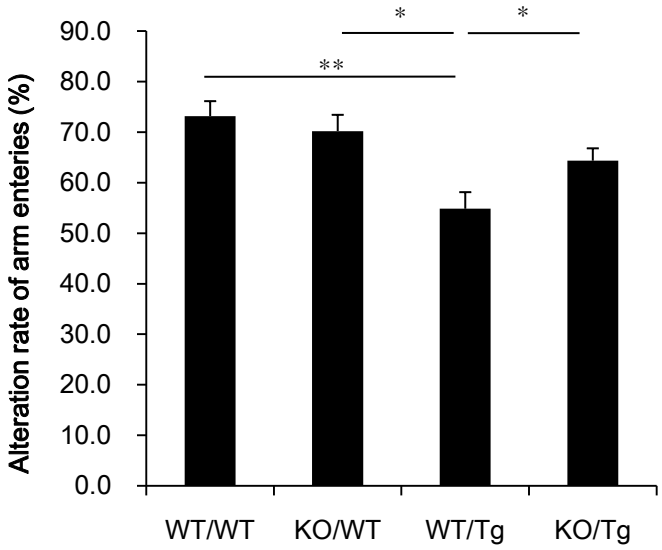

Figure 7. S100A9 KO/Tg crossbred mice showed significantly improvement in spatial memory.

In the Y-maze, the KO/Tg group showed a significant decrease in the alternation rate of arm entries. (n=9-11) $*P<0.05$, $**P<0.01$ by one-way ANOVA.

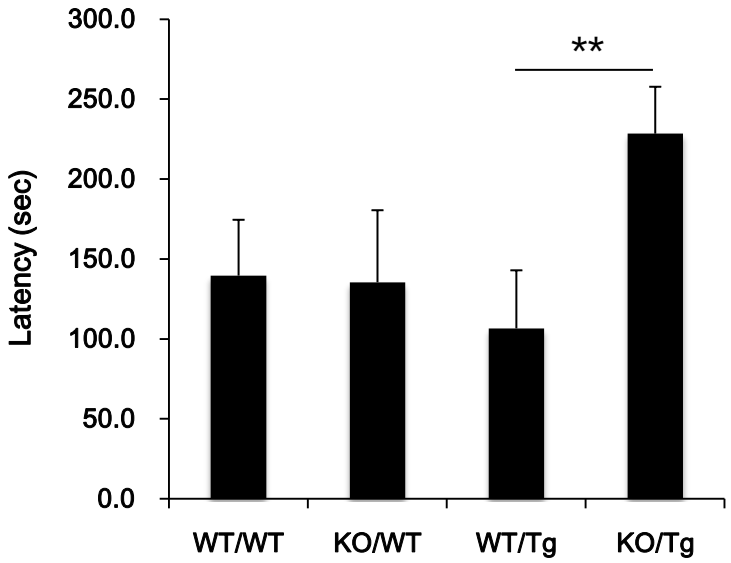

Figure 8. S100A9 KO/Tg crossbred mice showed significant improvement in learning and memory.

In the passive avoidance test, the latency time of the KO/Tg group was greatly increased. (n=11) $*P<0.05$, $**P<0.01$ by one-way ANOVA.

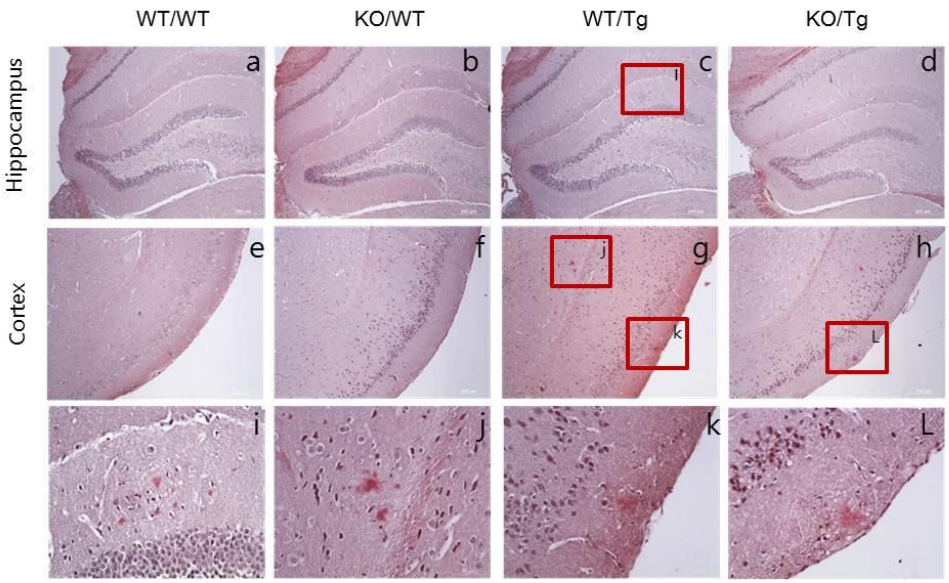

Figure 9. The number of amyloid plaques was reduced in S100A9 KO/Tg mice.

Histological analysis was performed out at the age of 14-months. In the cortex, hippocampus and entorhinal cortex, amyloid plaques were detected using Congo red staining. The Congo red-stained region of (c), (g) and (h). Sections are 4μm thick. ((a)-(h) Scale bar; 200 μm, (i)-(l) scale bar; 50 μm)

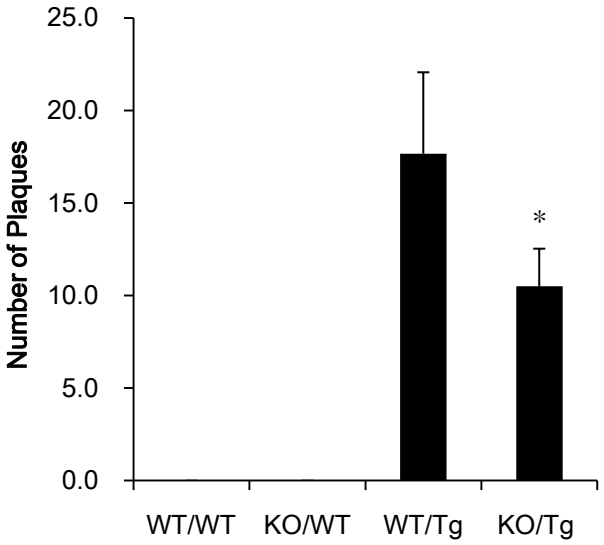

Figure 10. The quantitative analysis ofamyloid plaques was reduced in S100A9 KO/Tg mice.

Quantitative analysis of Congo red-stained plaque number. The number of amyloid plaques was counted in brain slices containing the hippocampal region of each group, and the average number of plaques per brain slice was calculated. In brains from the KO/Tg group, Aβwas significantly reduced in the cortex and hippocampus, compared to the WT/Tg group. The total numbers of mice per group were as follows: WT/WT (n=3), KO/WT (n=3), WT/Tg (n=6) and KO/Tg (n=6). $*P<0.05$ by one-way ANOVA.

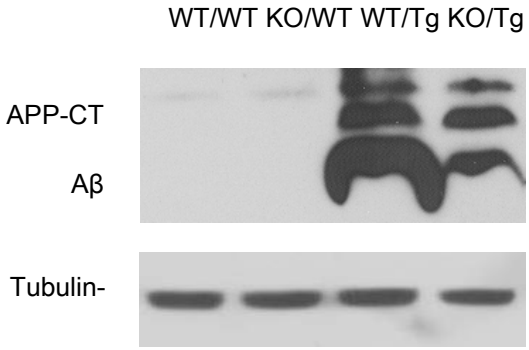

Figure 11. The amount of $A\beta_{1-42}$ was reduced in S100A9 KO/Tg mice.

Western blot analysis was performed with the total lysates from the cortical region and hippocampal region of brains in each group using the 6E10 antibody.

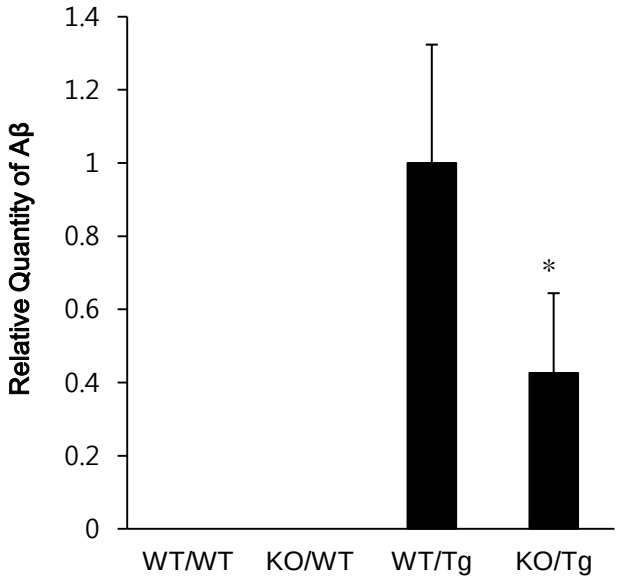

Figure 12. The relative quantity of $A\beta_{1-42}$ was reduced in S100A9 KO/Tg mice.

Aβ was detected and normalized by the amount of Tubulin. In the WT/Tg mice brain, Aβ was significantly produced compared to KO/Tg mice. (n=10)

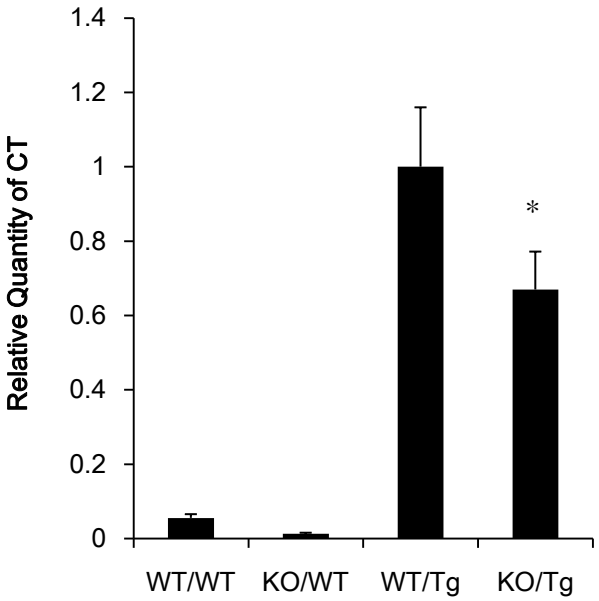

Figure 13. The relative quantity of APP-CT was reduced in S100A9 KO/Tg mice.

APP-CT was detected and normalized by the amount of Tubulin. In the WT/Tg mice brain, many APP-CT was produced compared to KO/Tg mice. (n=10)

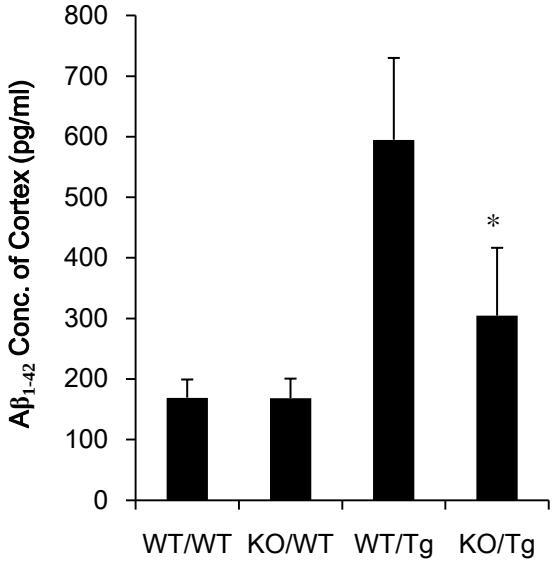

Figure 14. The levels of $A\beta_{1-42}$in cortical brain were reduced in S100A9 KO/Tg mice by Aβ ELISA.

$A\beta_{42}$ levels in cortical brain regions in all groups were analyzed by Aβ ELISA. The levels of $A\beta_{42}$ in the cortex of WT/Tg micewere highly increased in comparison to those of the age-matched WT/WT or WT/KO mice. Note that the levels of $A\beta_{42}$ were decreased in the cortex of KO/Tg mice brains compared with WT/Tg mice brains (n=4).

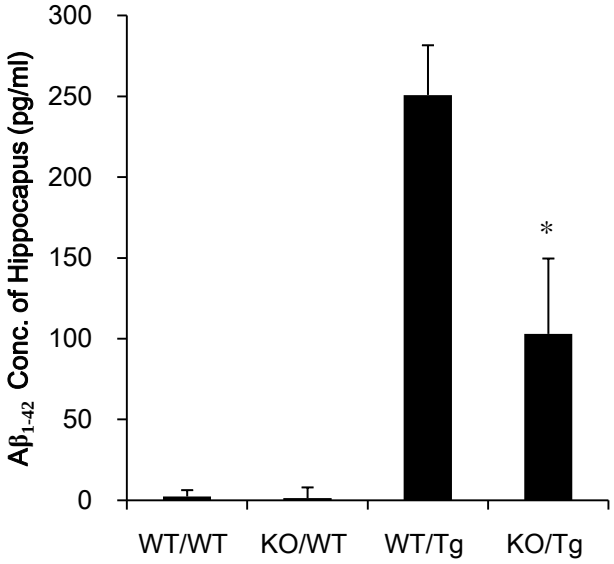

Figure 15. The levels of $A\beta_{1-42}$in hippocampal brain were reduced in S100A9 KO/Tg mice by Aβ ELISA.

$A\beta_{42}$ levels in hippocampal brain regions in all groups were analyzed by Aβ ELISA. The levels of $A\beta_{42}$ were significantly increased in the hippocampus of WT/Tg mice compared with age-matched WT/WT or WT/KO mice. Note that the levels of $A\beta_{42}$ were decreased in the hippocampus of KO/Tg mice brains compared with WT/Tg mice brains (n=4).

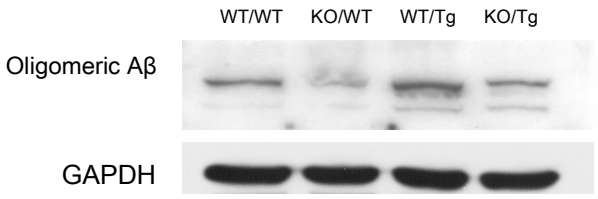

Figure 16. Theamount of oligomericAβ was reduced in S100A9 KO/Tgmice.

Western blot analysis was performed with total lysates from the cortical region of the brains in each group using an antibody against oligomeric Aβ.

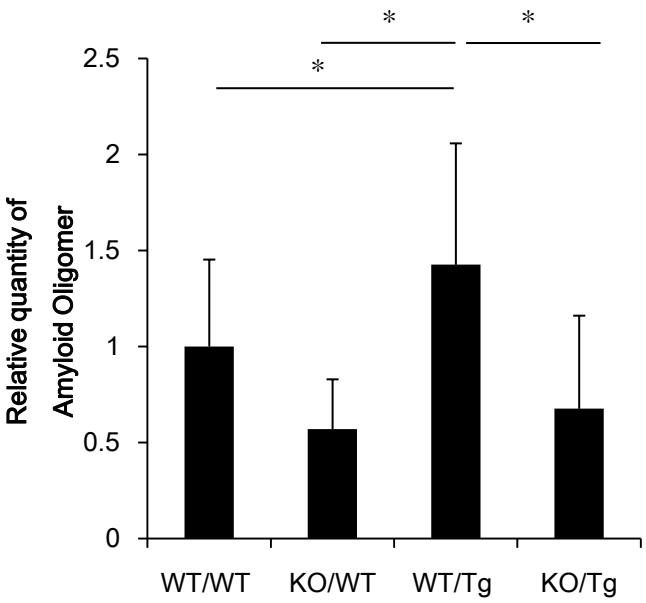

Figure 17. Therelative quantity of oligomericAβ was reduced in cortical brain of S100A9 KO/Tgmice.

In the cortex of KO/Tg mice brains, the relative quantity of oligomeric Aβ was decreased compared with WT/Tg mice. (n=3) $*P<0.05$ by one-way ANOVA.

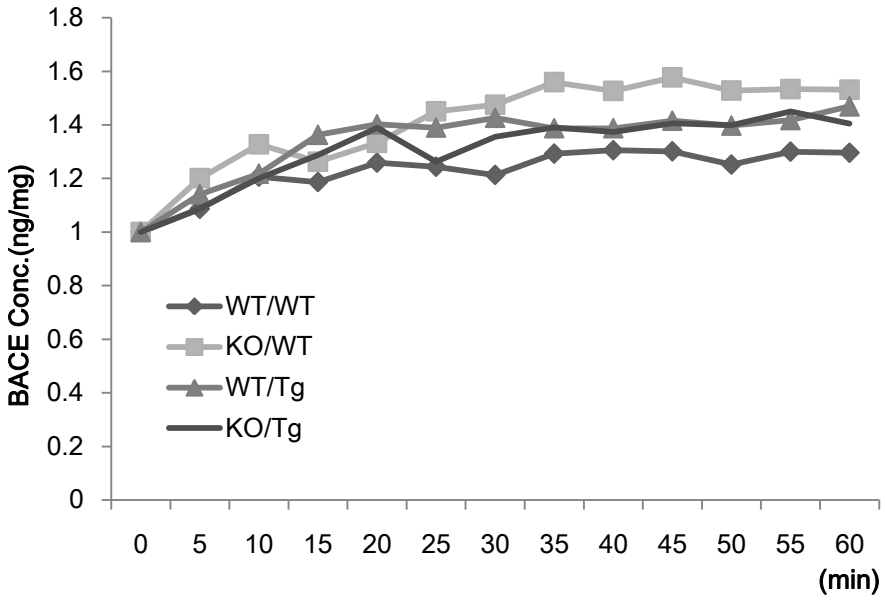

Figure 18. BACE activity in S100A9 KO/Tg mice

Enzymatic activity of the β-secretase from the mice brain lysates was assessed using fluorometric reaction. β-secretase activity was assessed as time passed. In S100A9 KO/Tg mice, significant changes in BACE activity were not detected . (n=6)

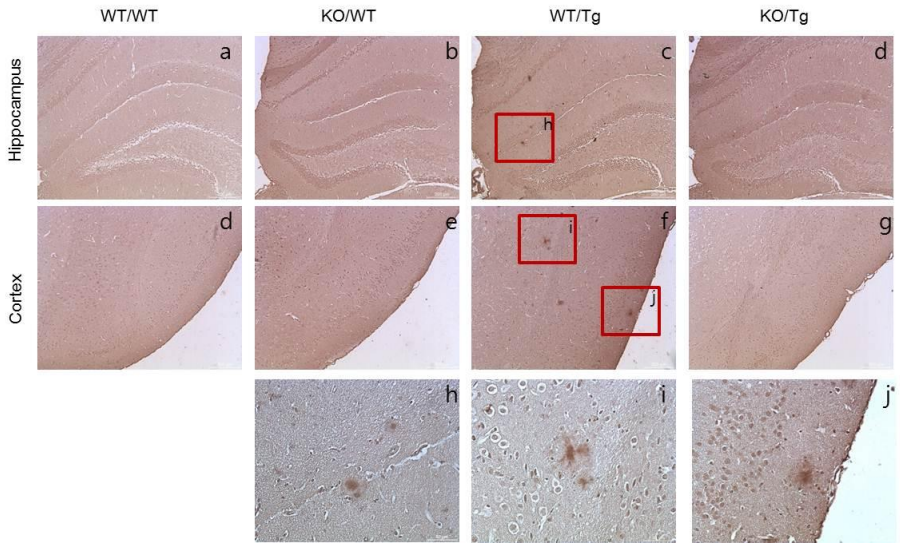

Figure 19. Accumulation of phosphorylated tau was detected in neurites surrounding amyloid plaques in the brain of S100A9 crossbred mice at 14 months old.

Phosphorylated tau (P-tau) was detected in the hippocampus and cortex of WT/Tg and KO/Tg mice brains by immunohistochemistry. The amount of P-tau was significantly reduced in KO/Tg mice brains compared with WT/Tg mice brains. (h)-(j) are P-tau stained region of (c) and (f). Sections are 4μm thick. ((a)-(g) Scale bar; 200 μm, (h)-(j) scale bar; 50 μm)

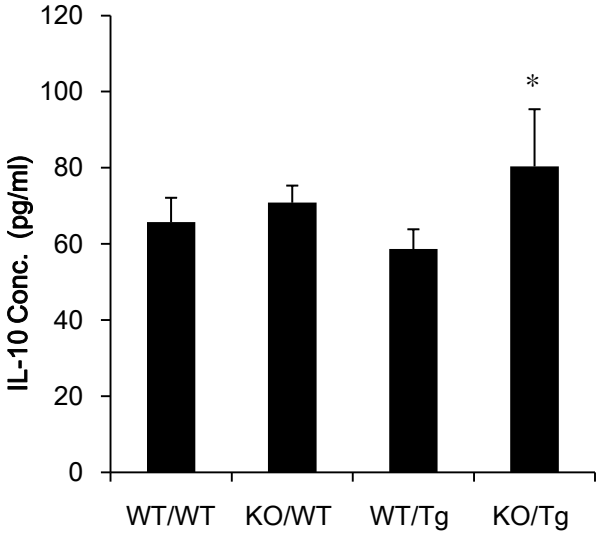

Figure 20. The anti-inflammatory cytokine IL-10 was significantly increased in the cortex of KO/Tg mice brains compared to WT/Tg mice brains at 14 months old.

The level of IL-10 was detected in the tissue lysates from the cortical region of the brain from each group by sandwich ELISA. IL-10, which is a representative anti-inflammatory cytokine, was increased in the cortex of KO/Tg mice brains compared to WT/Tg mice brains. (n=8), $*P<0.05$ by one-way ANOVA.

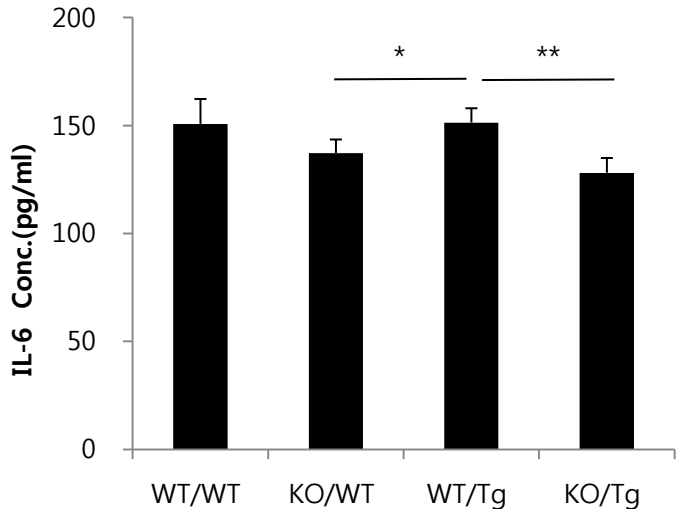

Figure 21. The pro-inflammatory cytokine IL-6 was significantly decreased in the cortex of KO/Tg mice brains compared to WT/Tg mice brains at 14 months old.

The level of IL-6 was detected in the tissue lysates from the cortical region of the brain from each group by sandwich ELISA. IL-6, which is a representative pro-inflammatory cytokine, was decreased in the cortex of KO/Tg mice brains compared to WT/Tg mice brains. (n=9-10), $*P<0.05$ by one-way ANOVA.

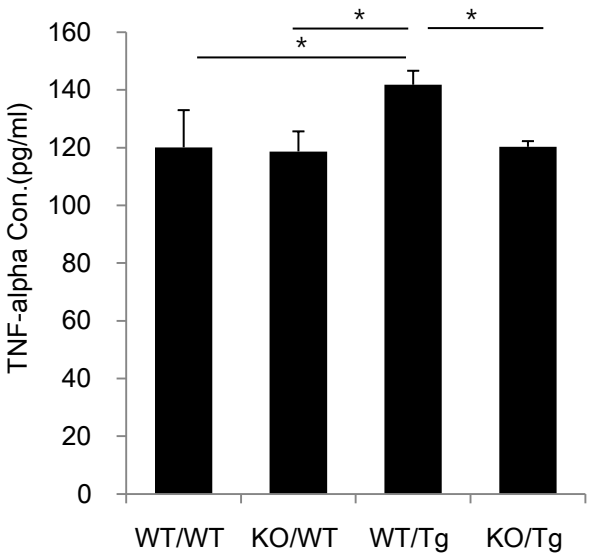

Figure 22. The pro-inflammatory cytokine TNF-α was slightly decreased in the cortex of KO/Tg mice brains compared to WT/Tg mice brains at 14 months old.

The level of TNF-α was detected in the tissue lysates from the cortical region of the brain from each group by sandwich ELISA. TNF-α, which is a representative pro-inflammatory cytokine, was decreased in the cortex of KO/Tg mice brains compared to WT/Tg mice brains. (n=8-10).

DISCUSSION

The S100A9 protein became the focus of current research because of its association with numerous human disorders, including acute and chronic inflammatory conditions, autoimmune diseases, cancer, atherosclerosis, cardiomyopathies and neurodegenerative diseases (2, 45,46), in addition to its crucial role in normal physiological processes within cells. Recently, S100A9 has been reported to participate in the inflammation of AD pathology (7, 8, 11). These studies support our hypothesis that knock out of the S100A9 gene in an AD mice model decreased memory impairment and AD-related pathogenesis as well as neurodegeneration.

To show the role of the S100A9 gene more clearly, I crossbred S100A9 KO mice and Tg2576 AD mice. I first confirmed knock-out of the S100A9 gene in the crossbred S100A9 KO and Tg2576 mice by genotyping, Western blot analysis and immunohistochemistry.

Deletion of S100A9 may result in a coordinate loss of S100A8 protein because of instability of S100A8 in the absence of its binding partner (S100A9) (30, 47, 48) therefore, I measured

the level of S100A8 in S100A9 KO mice. The mRNA levels and protein levels of S100a9 were reduced inthe cortex and hippocampus of APP-CT-Tg and age-matched WT mice brains (8). In our study, it was difficult to detect any differences in S100A8 expression from each group by Western blot analysis (Figure 3). In addition, I investigated the expression of other specific calcium-binding proteins, including Calnexin and S100B, in S100A9 KO/Tg crossbred mice brains. I confirmed Calnexin expression, which is a calcium-binding protein localized to the endoplasmic reticulum in S100A9 KO/Tg2576 crossbred mice. However, there was no difference in Calnexin expression (Figure 3). Overexpression of S100B in the mice brain is known to accelerate neurodegenerative disease pathology, including AD and PD (4, 49), and promote the synthesis of APP mRNA and APP in neurons, which could serve as a source of additional Aβ accumulation (50,51,52,53). In S100A9 KO/Tg2576 crossbred mice, each group did not show any differences in expression of the S100B protein (Figure 3). Our data indicate that the expression levels of S100A8, S100B, and Calnexin were not changed in S100A9 KO/Tg mice.

In AD animal mice, such as the Tg2576 mice, a rapid increase of Aβ begins at from 6 months, amyloid plaques are formed after 9−12 months, and memory deficits begin after 12 months (24,25,26,27).

I crossbred Tg2576 and S100A9 KO mice and investigated the behavioral and pathological characteristics of S100A9 KO/Tg2576 crossbred mice. Previous results have shown that S100A9 deficiency results in attenuated spatial learning and memory behavior in tests, including the Morris water maze, passive avoidance test, and Y−maze tasks, in 14−month−old mice. In our study, I found that S100A9 is related with learning and memory impairment in the AD mice model.

Spatial memory loss was related with the appearance of Aβ aggregates (27). Amyloid plaques and neurofibrillary tangles are believed to be the major pathological feature of AD (8,54,55). Our data showed that S100A9 KO/Tg mice have a decreased amyloid plaque load and tau pathology compared to S100A9 WT/Tg mice. The number of amyloid plaques and levels of monomeric and oligomeric Aβ were decreased in S100A9 KO/Tg mice. The total amount of $A\beta_{1-42}$ was greatly decreased in KO/Tg mice compared with WT/Tg mice. These

results raise the question that S100A9 may be involved in the formation of plaques and may contribute to Aβ aggregation. I previously showed that knockdown using short hairpin RNA reduced the amount of Aβ and APP-CT by decreasing BACE activity in Tg2576 mice. In S100A9 KO/Tg mice, significant changes in BACE activity were not detected (Figure 18).

In AD, tau is highly phosphorylated, which leads to the formation of neurofibrillary tangles. Phosphorylation of tau tends to provoke massive neuronal death and synaptic disruption. Therefore, I observed the level of phosphorylated tau in the brains of all mice groups. In the S100A9 KO/Tg group, tau phosphorylation was decreased. These results clearly showed beneficial pathological changes in the S100A9 KO/Tg mice.

Recent reports have shown that microglia in the brains of aged AD mice produced pro-inflammatory cytokines and S100A8 and S100A9 mRNA levels were significantly increased by stimulation of IL-6 and TNF-α (56). The anti-inflammatory cytokine IL-10 could inhibit the production of IL-6 and TNF-α (21). Based on these studies, I observed the levels of IL-10

in the brains of all mice groups and found that IL-10 expression was higher in KO/Tg mice compared to WT/Tg mice (Figure 20). As expected, expression of IL-6 and TNF-αin the brains were decreased in KO/Tg mice compared to WT/Tg mice (Figure 21 and 22). Therefore, the S100A9 deficiency-mediated cognitive improvements, and a reduction of AD pathology in AD models could be explained by the increased neuroprotective cytokine IL-10 and decreased inflammatory cytokines IL-6 and TNF-α.

I conclude that S100A9 KO dramatically improved the learning and memory function as well as the neuropathology of Tg2576 mice by diminishing the formation of amyloid plaques, decreasing Aβ and APP-CT levels and up-regulating cytokines such as IL-6, IL-10 and TNF-α. Thus, I suggest that S100A9 may be a potential therapeutic candidate for inflammatory-related AD.

REFERENCES

1. Fritz G, Botelho HM, Morozova-Roche LA, Gomes CM. Natural and amyloid self-assembly of S100 proteins: structural basis of functional diversity. The FEBS journal. 2010Nov; *277*, 4578-4590.

2. Salama I, Malone PS, Mihaimeed F, Jones JL. A review of the S100 proteins in cancer. Ejso-Eur J Surg Onc. 2008Apr; *34*, 357-364.

3. Boom A, Pochet R, Authelet M, Pradier L, Borghgraef P, Van Leuven F, Heizmann CW, Brion JP. Astrocytic calcium/zinc binding protein S100A6 over expression in Alzheimer's disease and in PS1/APP transgenic mice models. Bba-Mol Cell Res. 2004Dec; *1742*, 161-168.

4. Mori T, Koyama N, Arendash GW, Horikoshi-Sakuraba Y, Tan J, Town T. Overexpression of Human S100B Exacerbates Cerebral Amyloidosis and Gliosis in the Tg2576 Mouse Model of Alzheimer's Disease. Glia.

2010Feb; *58*, 300-314.

5. Mrak RE, Griffin WST. The role of activated astrocytes and of the neurotrophic cytokine S100B in the pathogenesis of Alzheimer's disease. Neurobiol Aging. 2001Nov-Dec; *22*, 915-922.

6. Roltsch E, Holcomb L, Young KA, Marks A, Zimmer DB.. PSAPP mice exhibit regionally selective reductions in gliosis and plaque deposition in response to S100B ablation. Journal of neuroinflammation. 2001May; *7*, 78.

7. Yanamandra K, Alexeyev O, Zamotin V, Srivastava V, Shchukarev A, Brorsson AC, et al. Amyloid formation by the pro-inflammatory S100A8/A9 proteins in the ageing prostate. PloS one. 2009 May; 4(5), e5562.

8. Ha TY, Chang KA, Kim JA, Kim HS, Kim S, Chong YH, Suh YH. S100a9 Knockdown Decreases the Memory Impairment and the Neuropathology in Tg2576 Mice, AD Animal Model. PloS one. 2010 Jan; 21;5(1):e8840.

9. Nacken W, Roth J, Sorg C, Kerkhoff C. S100A9/S100A8: Myeloid representatives of the S100 protein family as prominent players in innate immunity. Microscopy research and technique. 2003Apr;*60*, 569-580.

10. Nacken W, Mooren FC, Manitz MP, Bode G, Sorg C, Kerkhoff C. S100A9 deficiency alters adenosine-5'-triphosphate induced calcium signalling but does not generally interfere with calcium and zinc homeostasis in murine neutrophils. The international journal of biochemistry & cell biology. 2005Jun;*37*, 1241-1253.

11. Shepherd CE, Goyette J, Utter V, Rahimi F, Yang Z, Geczy CL, Halliday GM. Inflammatory S100A9 and S100A12 proteins in Alzheimer's disease. Neurobiol Aging. 2006Nov;*27*, 1554-1563.

12. Giannakopoulos P, Kovari E, Gold G, von Gunten A, Hof PR, Bouras C. Pathological substrates of cognitive decline in Alzheimer's disease. Front Neurol Neurosci.

2009Jan;*24*, 20-29.

13. Lee YJ, Han SB, Nam SY, Oh KW, Hong JT. Inflammation and Alzheimer's disease. Archives of pharmacal research. 2010Oct;*33*, 1539-1556.

14. Querfurth HW, Laferla FM. Alzheimer's Disease REPLY. New Engl J Med. 2010;*362*, 1844-1845.

15. Benilova I, Karran E, De Strooper B. The toxic Abeta oligomer and Alzheimer's disease: an emperor in need of clothes. Nature neuroscience. 2012Jan;*15*, 349-357.

16. Glabe CG. Structural Classification of Toxic Amyloid Oligomers. J Biol Chem. 2008Oct;*283*, 29639-29643.

17. Kayed R, Lasagna-Reeves C. Molecular Mechanisms of Amyloid Oligomers Toxicity. Journal of Alzheimer's disease. 2013;33 Suppl 1:S67-78.

18. Mc Donald JM, Savva GM, Brayne C, Welzel AT, Forster

G, Shankar GM, et al. The presence of sodium dodecyl sulphate-stable A beta dimers is strongly associated with Alzheimer-type dementia. Brain. 2010May;*133*, 1328-1341.

19. McLean CA, Cherny RA, Fraser FW, Fuller SJ, Smith MJ, Beyreuther K, et al. Soluble pool of Abeta amyloid as a determinant of severity of neurodegeneration in Alzheimer's disease. Annals of neurology. 1999Dec;*46*, 860-866.

20. Apelt J, Kumar A, Schliebs R. Age-related changes in neurotransmission in transgenic TG2576 mouse brain with neocortical beta-amyloid deposition. Journal of neurochemistry. 2001;*78*, 134-134.

21. Wilson EH, Wille-Reece U, Dzersznski F, Hunter CA. A critical role for IL-10 in limiting inflammation during toxoplasmic encephalitis. J Neuroimmunol. 2005Aug;*165*, 63-74.

22. Almeida CG, Tampellini D, Takahashi RH, Greengard P, Lin MT, Snyder EM, et al. Beta-amyloid accumulation in APP mutant neurons reduces PSD-95 and GluR1 in synapses. Neurobiology of disease. 2005Nov;*20*, 187-198.

23. Hsiao KK, Borchelt DR, Olson K, Johannsdottir R, Kitt C, Yunis W, et al. Age-related CNS disorder and early death in transgenic FVB/N mice overexpressing Alzheimer amyloid precursor proteins. Neuron. 1995 Nov;*15*, 1203-1218.

24. Hsiao K, Chapman P, Nilsen S, Eckman C, Harigaya Y, Younkin S, et al. Correlative memory deficits, A beta elevation, and amyloid plaques in transgenic mice. Science. 1996 Oct;*274*, 99-102.

25. Irizarry MC, McNamara M, Fedorchak K, Hsiao K, Hyman BT. APPSw transgenic mice develop age-related A beta deposits and neuropil abnormalities, but no neuronal loss in CA1. Journal of neuropathology and

experimental neurology. 1997 Sep;*56*, 965-973.

26. Kawarabayashi T, Younkin LH, Saido TC, Shoji M, Ashe KH, Younkin SG. Age-dependent changes in brain, CSF, and plasma amyloid beta protein in the Tg2576 transgenic mouse model of Alzheimer's disease. Journal of Neuroscience. 2001 Jan;*21*, 372-381.

27. Westerman MA, Cooper-Blacketer D, Mariash A, Kotilinek L, Kawarabayashi T, Younkin LH, et al. The relationship between Abeta and memory in the Tg2576 mouse model of Alzheimer's disease. The Journal of neuroscience : the official journal of the Society for Neuroscience. 2002 Mar;*22*, 1858-1867.

28. Chen G, Chen KS, Knox J, Inglis J, Bernard A, Martin SJ, et al. A learning deficit related to age and beta-amyloid plaques in a mouse model of Alzheimer's disease. Nature. 2000 Dec;*408*, 975-979.

29. Janus C, Pearson J, McLaurin J, Mathews PM, Jiang Y,

Schmidt SD, et al. A beta peptide immunization reduces behavioural impairment and plaques in a model of Alzheimer's disease. Nature. 2000 Dec;*408*, 979-982.

30. Manitz MP, Horst B, Seeliger S, Strey A, Skryabin BV, Gunzer M, et al. Loss of S100A9 (MRP14) Results in Reduced Interleukin-8-Induced CD11b Surface Expression, a Polarized Microfilament System, and Diminished Responsiveness to Chemoattractants In Vitro. Molecular and Cellular Biology. 2003 Feb;*23*, 1034-1043.

31. Jung BK, Pyo KH, Shin KY, Hwang YS, Lim H, Lee SJ, et al. Toxoplasma gondii Infection in the Brain Inhibits Neuronal Degeneration and Learning and Memory Impairments in a Murine Model of Alzheimer's Disease. PloS one. 2012;*7*, e33312.

32. Shen Z, Wang G, Lin SZ. Two-way shuttlebox avoidance conditioning and brain NADH in rats. Physiology & behavior. 1990 Oct;*48*, 515-517.

33. Shin KY, Lee GH, Park CH, KimHJ, Park SH, Kim S, et al. A novel compound, maltolyl p-coumarate, attenuates cognitive deficits and shows neuroprotective effects in vitro and in vivo dementia models. J Neurosci Res. 2007 Aug;*85*, 2500-2511.

34. Avila J, Lim F, Moreno F, Belmonte C, Cuello AC. Tau function and dysfunction in neurons: its role in neurodegenerative disorders. Molecular neurobiology. 2002 Jun;*25*, 213-231.

35. Buee L, Bussiere T, Buee-Scherrer V, Delacourte A, Hof PR. Tau protein isoforms, phosphorylation and role in neurodegenerative disorders. Brain research. Brain research reviews. 2000 Aug;*33*, 95-130.

36. Ferrer I, Gomez-Isla T, Puig B, Freixes M, Ribe E, Dalfo E, et al. Current advances on different kinases involved in tau phosphorylation, and implications in Alzheimer's disease and tauopathies. Current Alzheimer research.

2005 Jan;*2*, 3-18.

37. Lee VM, Goedert M, Trojanowski JQ. Neurodegenerative tauopathies. Annual review of neuroscience. 2001;*24*, 1121-1159.

38. Spillantini MG, Goedert M. Tau protein pathology in neurodegenerative diseases. Trends in neurosciences. 1998 Oct;*21*, 428-433.

39. Higgins LS, Holtzman DM, Rabin J, Mobley WC, Cordell B. Transgenic mouse brain histopathology resembles early Alzheimer's disease. Annals of neurology. 1994 May;*35*, 598-607.

40. Masliah E, Sisk A, Mallory M, Games D. Neurofibrillary pathology in transgenic mice overexpressing V717F beta-amyloid precursor protein. Journal of neuropathology and experimental neurology. 2001 Apr;*60*, 357-368.

41. Sturchler-Pierrat C, Abramowski D, Duke M, Wiederhold KH, Mistl C, Rothacher S, et al. Two amyloid precursor protein transgenic mouse models with Alzheimer disease-like pathology. Proceedings of the National Academy of Sciences of the United States of America. 1997 Nov;*94*, 13287-13292.

42. Tomidokoro Y, Harigaya Y, Matsubara E, Ikeda M, Kawarabayashi T, Shirao T, et al. Brain A beta amyloidosis in APPsw mice induces accumulation of presenilin-I and tau. J Pathol. 2001 Aug;*194*, 500-506.

43. Mellins ED, Macaubas C, Grom AA. Pathogenesis of systemic juvenile idiopathic arthritis: some answers, more questions. Nat Rev Rheumatol. 2011 Jun;*7*, 416-426.

44. Mehlhorn G, Hollborn M, Schliebs R. Induction of cytokines in glial cells surrounding cortical beta-amyloid plaques in transgenic Tg2576 mice with Alzheimer pathology. Int J Dev Neurosci. 2000Jul-Aug;*18*, 423-

431.

45. Hoyaux D, Decaestecker C, Heizmann CW, Vogl T, Schafer BW, Salmon I, et al. S100 proteins in Corpora amylacea from normal human brain. Brain research. 2000 Jun;*867*, 280-288.

46. Van Lent PL, Grevers L, Blom AB, Sloetjes A, Mort JS, Vogl T, et al. Myeloid-related proteins S100A8/S100A9 regulate joint inflammation and cartilage destruction during antigen-induced arthritis. Annals of the rheumatic diseases. 2008 Dec;*67*, 1750-1758.

47. Loser K, Vogl T, Voskort M, Lueken A, Kupas V, Nacken W, et al. The Toll-like receptor 4 ligands Mrp8 and Mrp14 are crucial in the development of autoreactive CD8+ T cells. Nature medicine. 2010 Jun;*16*, 713-717.

48. Vogl T, Tenbrock K, Ludwig S, Leukert N, Ehrhardt C, van Zoelen MA, et al. Mrp8 and Mrp14 are endogenous activators of Toll-like receptor 4, promoting lethal,

endotoxin-induced shock. Nature medicine. 2007 Sep;*13*, 1042-1049.

49. Liu JL, Wang HL, Zhang LF, Xu YF, Deng W, Zhu H, et al. S100B Transgenic Mice Develop Features of Parkinson's Disease. Arch Med Res. 2011 Jan;*42*, 1-7.

50. Li CY, Zhao R, Gao K, Wei Z, Yin MY, Lau LT, et al. Astrocytes: Implications for Neuroinflammatory Pathogenesis of Alzheimer's Disease. Current Alzheimer research. 2011 Feb;*8*, 67-80.

51. Li Y, Wang J, Sheng JG, Liu L, Barger SW, Jones RA, et al. S100 beta increases levels of beta-amyloid precursor protein and its encoding mRNA in rat neuronal cultures. Journal of neurochemistry. 1998 Oct;*71*, 1421-1428.

52. Liu L, Li Y, Van Eldik LJ, Griffin WS, Barger SW. S100B-induced microglial and neuronal IL-1 expression is mediated by cell type-specific transcription factors. Journal of neurochemistry. 2005 Feb;*92*, 546-553.

53. Sheng JG, Mrak RE, Griffin WST. Glial-neuronal interactions in Alzheimer disease: Progressive association of IL-1 alpha(+) microglia and S100 beta(+) astrocytes with neurofibrillary tangle stages. Journal of neuropathology and experimental neurology. 1997 Mar;*56*, 285-290.

54. Selkoe DJ. Alzheimer's disease results from the cerebral accumulation and cytotoxicity of amyloid beta-protein. Journal of Alzheimer's disease : JAD. 2001 Feb;*3*, 75-80.

55. Suh YH, Checler F. Amyloid precursor protein, presenilins, and alpha-synuclein: Molecular pathogenesis and pharmacological applications in Alzheimer's disease. Pharmacol Rev. 2002 Sep;*54*, 469-525.

56. Eggers K, Sikora K, Lorenz M, Taubert T, Moobed M, Baumann G, et al. RAGE-Dependent Regulation of Calcium-Binding Proteins S100A8 and S100A9 in Human THP-1. Exp Clin Endocr Diab. 2011 Jun;*119*,

353-357.

국문초록

염증관련 S100A9 유전자가 알츠하이머병 모형 마우스와 알츠하이머병 환자에서 상당히 증가된다는 것을 지난 연구를 통해 확인하였다. 게다가 S100A9의 발현을 감소시킨 경우 알츠하이머병 동물 모델인 Tg2576마우스에서 인지 기능이 증가하는 것과 아밀로이드플라크가 감소되는 것을 확인하였다.

알츠하이머병에서의 S100A9의 발병과 진행에 관한 영향을 확인하기 위하여 알츠하이머병 동물 모델인 Tg2576마우스와 S100A9의 KnockOut(KO) 마우스의 형질교배를 통해 새로운 동물 모형을 제작하였다. 이를 통해 S100A9 KO/Tg2576 (KO/Tg) 마우스를 동일한 나이에서의 S100A9 WT/Tg2576 (WT/Tg)와 비교하였을 때, 공간 지각력 확인을 위한 수중미로테스트, 공간 기억 확인을 위한 Y-미로테스트, 기억과 학습에 대한 효과를 알아보기 위한 수동회피반응을 통해 공간 인지 기억력의 증가를 확인하였다. 또한, 아밀로이드베타(Aβ)와 C단단백질(APP-CT), 인산화된 타우 (phosphorylated tau)의 레벨 감소, 그리고 인터루킨-10(IL-10)의 레벨을 증가를 확인하였다.

이러한 결과는 S100A9이 Tg2576에서 나타나는 신경퇴행 및 인지 장애에 관하여 작용하는 것으로 보인다. S100A9의 작용 기작은 염증 과정과 관련이 있는 것으로 보인다. 이러한 발견은

S100A9의 knockout이 알츠하이머병의 약리학적 치료의 주요한 타겟으로 작용할 것이라는 것을 보여준다.

주요어: 알츠하이머병, S100A9, Knockout, 염증

학 번: 2010-30608